

# **CHAPTER 5**

*Applicability of Cerium (IV) and Thorium (IV)  
Phosphates as Solid State Proton Conductors*

---

## 5.1 INTRODUCTION

Solid state ionics is an interdisciplinary science which covers physics, chemistry and materials science, both fundamental and applied, involved all kinds of ionic transport in solid state. Solid electrolytes are a class of solid substances that conduct electric current by ionic motion (as do electrolyte solutions, e.g. aqueous solution of sodium chloride).

In solid electrolytes, ions are not fixed at the lattice points, but are more or less mobile from lattice point to lattice point or from lattice point to an interstitial position. When an electric field is applied, such ions moving about the crystal at random, migrate along the direction of electric field. This phenomenon is ionic conduction, expressed as, ionic conductivity ( $\sigma$ ) =  $\sum \sigma_i = \sum n_i e_i \mu_i$ , where  $n_i$  = number of charge carriers of species  $i$ ,  $e_i$  = charge on such a carrier and  $\mu_i$  = mobility.

Solid electrolytes are lately the focus of much attention. Although the presence of ionic conductivity in solids has been recognized since the end of the nineteenth century, the interest towards solid fast ion conductors has grown markedly since 1960s and increased considerably in the last decade in view of their possible application in solid state electrochemical devices for energy conversion and storage and environmental monitoring.

Material diversity is also an important feature of solid state ionics. Solid state ionics involves materials of varied morphology, including single crystals, sintered bodies, composites and even amorphous thin films. When selecting materials for device applications, the intended operating temperature and thermal stability of the ion conductor are very significant considerations. Industrial applications for solid electrolytes include fuel cells e.g. producing electricity by electrochemical reaction of hydrogen and oxygen, and sensors (for analytical determination of gases such as hydrogen and oxygen), photo cells, electrochromic display, and secondary (rechargeable) battery. They can be built into a solid state device, which are stable, reliable and easy to operate in the above mentioned applications. Solid state electrochemical devices are operated either with high current densities (electrolysers, batteries) or at very low current (electrochemical sensors, memories, electrochemical devices etc.). In order to find application in electrochemical device, a solid electrolyte should have conductivity of at least  $10^{-3} \text{ Scm}^{-1}$  at the working temperature.

## 5.2 CRITERIA FOR ION CONDUCTION IN SOLID ELECTROLYTES

A set of requirements for a material to be a potential ion conductor has been set out[1] as follows:

- A large number of potential charge carriers/mobile ions.
- An excess of acceptable sites for mobile ions.
- A small energy difference between ordered and disordered distributions of mobile ions in the material structure
- A low activation barrier for the motion of charge carriers between sites.
- A rigid framework structure through which the ions can migrate.
- A highly polarizable framework.
- Thermal and chemical stability in the intended device environment.

## 5.3 CRITERIA FOR HIGH IONIC MOBILITY

Ionic conductivity in solid electrolytes depends on the number of conducting ions as well as their mobility. Following are the criteria considered for high ionic mobility.

**Ionic radii and charge:** Smaller cations can move more freely compared to larger anions in a lattice. Most of the superionic materials developed so far are for monovalent cationic conductors. Dunn and Farrington [2] have reported a few materials showing high mobility at high temperatures for divalent cation  $Ba^{2+}$ ,  $Cd^{2+}$ ,  $Sr^{2+}$ . However, the mobility of divalent cations is much less compared to monovalent ions. This may be due to the fact that coulombic energies involved in jumping/hopping for di-or-trivalent ions is greater than that for monovalent ions.

**Lattice interaction:** An important criterion is that the mobile ions should be weakly bound to the rigid lattice. Smaller ions are bonded more strongly to the lattice, at the same time, small ionic radii would permit a greater ease in its movement. Therefore, in most materials, a compromise has to be struck between both these effects which control the net mobility. For example,  $Li^+$  ion in  $Li-\beta$  alumina despite its small ionic radii or size, is much less mobile than  $Na^+$  in  $Na-\beta$  alumina, apparently as a consequence of a weaker  $Na-O$  bond [3].

**Ion polarisability:** Diffusion through the faces of the coordination polyhedron is made easier by the large polarisability of the mobile species as well as that of ion on

the lattice. The latter possibly distorts an electron cloud during movement of the mobile ion. Analysis of the electronic properties of various fluorides crystallizing with the same structure shows that larger the polarisability of the cations, the greater is the ionic conductivity [4].

**Coordination number of mobile species:** Fast ionic mobility is easier for mobile species with low coordination number. For example, in NaF, CaF<sub>2</sub> and LaF<sub>3</sub> the coordination numbers of fluorine ions are 6, 4 and 3 respectively, and consequently their conductivities are in the order,  $\sigma_{\text{NaF}} < \sigma_{\text{CaF}_2} < \sigma_{\text{LaF}_3}$ . In some silver conductors, good ionic conductivity is observed due to lower coordination numbers (4, 3 or 2) of Ag<sup>+</sup> in the equilibrium positions [5]. However, AgF, AgCl, AgBr exhibit poor conductivity due to high coordination number (6) of Ag<sup>+</sup>.

**Structure and concentration of mobile ion:** Greater the number ( $n$ ) of mobile ions, higher will be the conductivity ( $\sigma$ ). Disorder in structure, generally increases  $n$  and  $\mu$ . For high mobility, the energy difference of the cation-anion interactions, in the various sites involved should be small, additionally there must be a sufficient number of vacant sites for an ion to hop/jump. Structure is probably the most important factor responsible for high ionic conduction. A highly ‘disordered structure’ which means that, the number of sites in the cationic sublattice is more than the number of cations in the unit cell, is the common factor in all the high conducting materials. Here, the percentage occupancy of each site is low, so hopping of ions from one site to another may take place freely, giving high conduction. One typical example is  $\alpha$ -AgI, where the number of sites per unit cell is twelve as against two silver ions. So, the two Ag<sup>+</sup> ions can jump freely into the twelve sites available in that unit cell.

## 5.4 TYPES OF SOLID ELECTROLYTES

Materials that can function as ion conductors include crystalline solids, amorphous materials, glasses, polymers and ceramics. Depending on the ions which are responsible for the conduction property, solid electrolytes can be categorized as follows [6].

**Oxide ion conductors:** This class basically includes compounds of Fluorite type solid solutions (ZrO<sub>2</sub> -CaO, ZrO<sub>2</sub> -Y<sub>2</sub>O<sub>3</sub>, ThO<sub>2</sub> -Y<sub>2</sub>O<sub>3</sub>, CeO<sub>2</sub> - La<sub>2</sub>O<sub>3</sub> etc.) and compounds based on Bi<sub>2</sub>O<sub>3</sub>. The conductivity in these solid electrolytes is mainly due to two

contributions: a) association of vacancies ( $V_{\text{O}}$ ) or formation of defect pairs and b) formation of super lattice or ordering of vacancies.

**Fluoride ion conductors:** It includes Fluorite type fluorides and rare earth fluorides. In Fluorite type fluorides,  $F^-$  conducts through its vacancies ( $V_{F^-}$ ) generated by the partial replacement of high valency cation with a monovalent cation such as  $Na^+$ . In rare earth fluorides, at low temperatures,  $F^-$  conduction takes place via Schottky-type defects.

**Silver and Copper conductors:** They include the halides, complex salts based on halides and conductive glasses. In case of halides, ionic conduction is observed due to “Structural Disorder” originating in its crystallographic nature. In case of complex salts, based on halides, the conductivity is mainly due to a structure based on connected tetrahedral anions. The conduction mechanism of conductive glasses is still not clear, but it is observed that their conductivities are reduced by three orders of magnitude on crystallization at high temperatures. Hence, the high conductivity in such glasses is due to their glassy or amorphous structure itself.

**Lithium ion conductors:** It includes lithium halide based materials, lithium nitride ( $Li_3N$ ) and its derivatives, oxoacid salts and solid polymer electrolytes. In lithium halide based materials, the conduction can be explained to be due to the space charge layer, consisting of  $V_{Li}$  or  $Li^+$  generated at the interface between the host and the dielectric particles. In case of  $Li_3N$  and its derivatives, the mechanism is not clear and reported conductivities differ, depending on the synthesis condition and sample history. However, impurities when doped, affect the conductivities. It has been observed that when  $Li_3N$  was doped with hydrogen, results in a higher conductivity value. The oxoacid salts exhibit conductivity due to the movement of  $Li^+$  via the vacant interstices in the a-b plane of an orthorhombic system, in which oxygen ions are packed into hcp array. In case of polymer electrolytes, an amorphous composite phase, behaving like a solution, at a temperature higher than glass transition temperature, is mainly responsible for conduction.

**Sodium and Potassium ion conductors:** It includes  $\beta$ -alumina,  $\beta$ -alumina incorporated with multivalent cations, NASICON (Na super ion conductor) and related oxoacid salts and Hollandites ( $Ba_xMn_8O_{16,x} \leq 2$ ). Ionic conduction in  $\beta$ -alumina is due to the “half-fused” state of  $Na^+$  lattice and takes place along a plane sandwiched by spinel layers. In NASICON, the significant conduction is mainly due to the “partial occupation” of available sites by  $Na^+$ .

***Proton conductors:*** Proton conductors are a special class of solid electrolytes, where hydrogen ions are the primary charge carriers. Proton conductors are often considered to be electrolytes in which hydrogen is transported towards and evolved at the cathode during electrolysis.

***The present study involves the application of TMA salts as solid state proton conductors. Therefore proton conductors are discussed in detail.***

## **5.5 MECHANISM OF PROTON CONDUCTION**

An electrical charge carrier in solids is generally divided into two classes, ions or electrons. Ions are relatively massive and ion transport is often described by a “hopping” mechanism of the ion from site to site. On the other hand, electron motion in metals and broad band semiconductors is described quantum mechanically. The proton, small but massive compared to the electron, lies between these two extremes and consequently, there is special interest in examining its behaviour as a charge carrier in solids with the possible requirement of quantum descriptions in some situations and particle description in others.

Water is a good conductor of protons, because of the H-bonded networks between water molecules that give water its liquid properties in the physiological range. In ice, the H-bonded networks are more extensive, and ice is a better conductor than liquid water. Conduction in ice occurs through a "hop-turn" mechanism, first suggested by Grotthuss, and often referred to as the Grotthuss mechanism (**Figure 5.1**).

In the "hop" part of the mechanism, a proton first hops from the end of the H-bonded chain to an adjacent group (I, right); transfer of H-bond strength then allows it to be replaced by H<sup>+</sup> binding at the other end, to give the structure in II. In the "turn" phase, rotation of the water as shown in II then restores the starting structure (I).

Proton transport includes, transport of proton (H<sup>+</sup>) and any assembly that carries protons (OH<sup>-</sup>, H<sub>2</sub>O, H<sub>3</sub>O<sup>+</sup>, NH<sub>4</sub><sup>+</sup>, HS<sup>-</sup> etc). The transport of protons (H<sup>+</sup>) between relatively stationary host anions is termed the ‘Grotthuss’ or ‘free-proton’ mechanism [7]. The Grotthuss mechanism requires close proximity of water molecules, which are firmly held but able to rotate. The activation energy is thus low, since it depends entirely on the reorientation step [8]. Transport by any other species is termed as “Vehicle mechanism” [9]. Here, the polyatomic ion such as H<sub>3</sub>O<sup>+</sup>, OH<sup>-</sup> or

$\text{NH}_4^+$  migrates as entities through the bulk materials. Thus, the activation energy is expected to be high. A pictorial representation of Grotthuss and Vehicle mechanism are presented in **Figure 5.2 and 5.3** respectively.

Vehicle mechanism is most frequently encountered in aqueous solution and other liquid/melts. However, in solids, vehicle mechanism is usually restricted to materials with open structures (channels, layers) to allow passage of the large ions and molecules. Compounds with less amount of water would be expected to conduct by vehicle mechanism, in which a nucleophilic group such as  $\text{H}_2\text{O}$  or  $\text{NH}_3$  acts as a proton carrier.

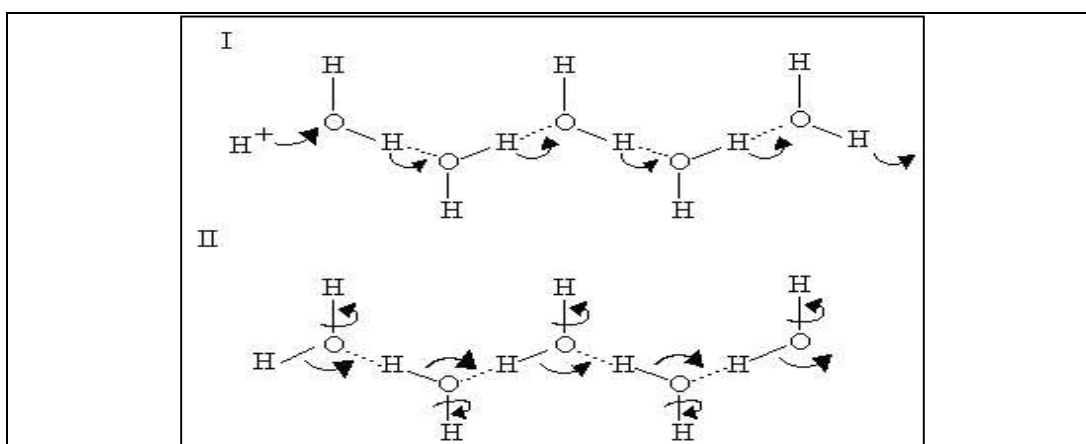


**Figure 5.1** Proton conduction by Grotthuss mechanism

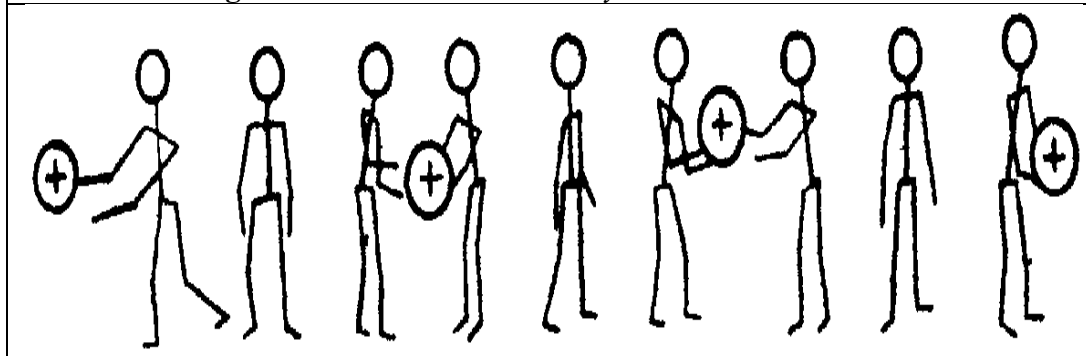


**Figure 5.2** Cooperative ion motion with reorientation and hopping (Grotthuss) mechanism

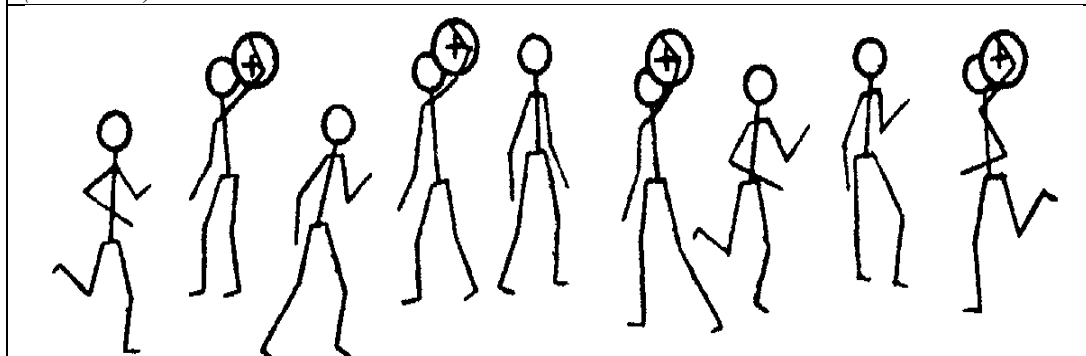


**Figure 5.3** Poly atomic ion transport (vehicle mechanism)

For materials that adopt Grotthuss mechanism, a major shortcoming is that they require water for ion conduction. At higher temperature due to dehydration, when this water is lost, the conductivity decreases by several orders of magnitude.

The transport of proton can be either a bulk phenomenon or a surface dominated process. Cesium phosphate is a good example of compounds showing bulk conduction mechanism [10-11]. At room temperature, it has a monoclinic structure, however, upon heating through 141 °C it undergoes a phase change to tetragonal. This phase change is accompanied by an increase in the conductivity by two or three orders of magnitude and is often referred to as a “Superprotonic” transition [12].

In  $\alpha$ -ZrP, the water molecule is hydrogen bonded to two of the phosphate protons and forms a hydrogen bond as donor to a third phosphate group [13, 14]. There is no evidence of presence of hydronium ion. Thus, conduction in the interior of the crystal must occur by a modified vehicle mechanism as rotation of the water molecule is difficult. It is proposed that the high conductivity is due to the ability of water located there to rotate and participate in Grotthuss-type transport aided by water sorbed on the surface. Thus, the transport mechanism in  $\alpha$ -ZrP at room temperature is dominated by surface transport [15, 16]. Alberti and coworkers have also shown that the surface conducts protons thousand times faster than the bulk protons [17]. However, at higher temperature ( $> 120$  °C), the conduction is essentially due to bulk protons [18]. At this temperature, solid being anhydrous and the protons being covalently bonded to phosphate [13], conduction of protons require breaking and making of bonds (**Figure 5.4**). Thus, conduction decreases with increase in temperature.

The ideal situation for good conductivity is that charge carriers should be trapped within the cavities where transport of protons from one end of the cavity to the other, utilize the framework for hopping of the proton. Judicious framework substitutions have achieved this effect. In each of the phosphate group in  $\alpha$ -ZrP there is single oxygen pointing into the interlamellar region and carries a full negative charge. Therefore, this oxygen forms a strong covalent bond with the proton, which, in crystals, does not form hydronium ion in the monohydrate phase. In general, in the oxyanion framework structure, the metal of the oxyanion must have the highest possible charge and be surrounded by the maximum number of oxygen ions. This results in charge distribution thereby making the attraction for a proton weak.

Therefore, in the presence of water, hydronium ions are formed readily and the material results in a strong acid and excellent conductor.

Transport between two water molecules is generally a result of protonic defects and occurs through the breaking and reformation of bonds. This is caused because the proton defect weakens the intermolecular interactions which cause large variations in bond length combined with rapid breaking and forming of bonds as shown in **Figure 5.4** [10, 19, 20].

In surface functionalized metal (IV) phosphate, transport occurs along the exposed acid sites on the surface which are either involved in the interaction themselves or responsible for water domains within the structure that promotes transport of protons. This water assisted transport which is likely to be more dominant, is shown in **Figure 5.5** [21].

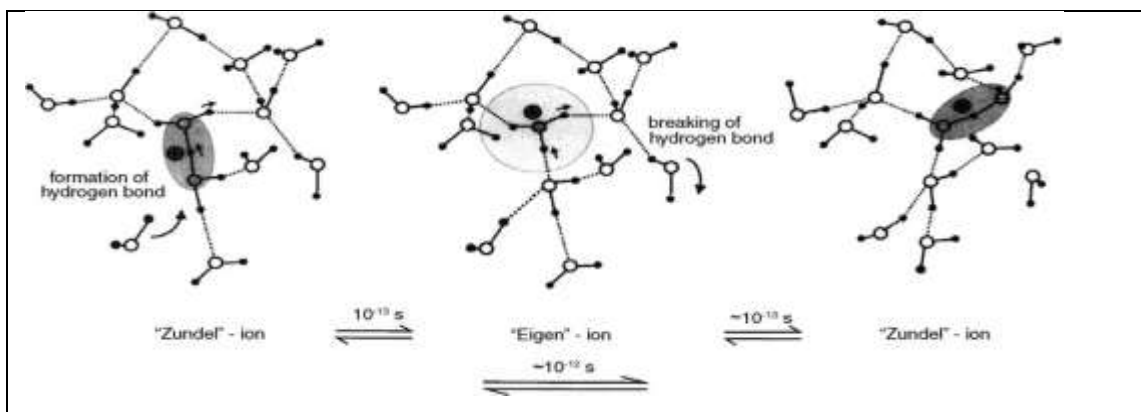


**Figure 5.4** Transport Mechanism of a protonic defect in water [10]

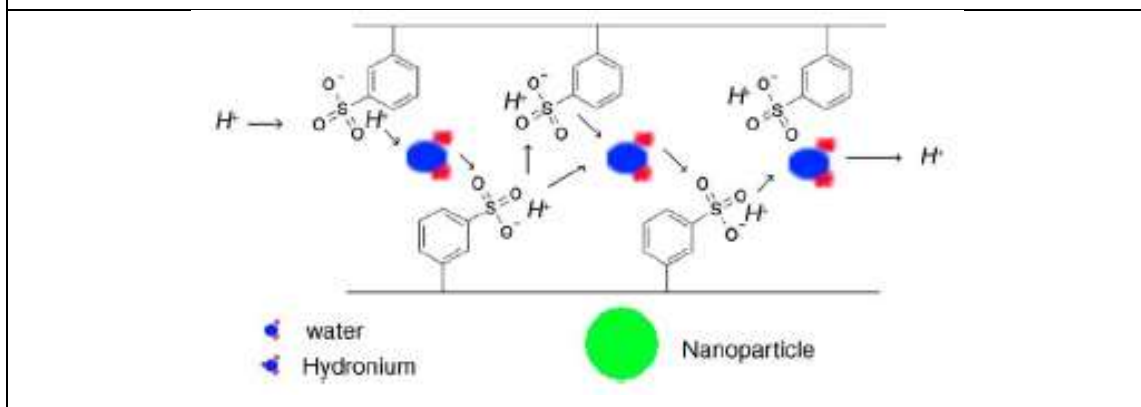


**Figure 5.5** Proton transport in surface functionalized solid acid membranes [21]

Proton conduction differs from the conduction of other ions ( $\text{Na}^+$ ,  $\text{K}^+$ ,  $\text{Ag}^+$ ) principally in a way, hydrogen bond is covalent and directional in character whereas metal ions in ionic solids experience coulombic forces more or less from all sides.

In the literature cited above, one evidence that has come forth is that the proton conductivity strongly depends on water stoichiometry. The best proton conductors usually contain water molecules as an essential constituent

## **5.6 LIMITATIONS OF PROTON CONDUCTORS**

Criteria for high conductivity i.e. monovalent and small ionic radii are satisfied in case of  $H^+$  ion, yet not many good proton conductors are available. Some problems associated with proton conduction are listed below [8]:

- Charge to mass ratio is high in case of hydrogen; hence it is strongly bound to the lattice/tightly attached to the lattice.
- Naked  $H^+$  are not found in solids under equilibrium condition (half life ( $\tau$ )  $> 10^{-11}$  sec).  $H^+$  is always covalently bonded to some electronegative atoms/ions in the structure e.g. C–H, N–H, O–H.
- Protons can be shared between two electronegative atoms e.g. O–H–O. This is the so-called hydrogen bond.
- Oscillation of H from one side to the other in a hydrogen bond O–H–O $\leftrightarrow$ O–H–O corresponds to a net transport of charge and is therefore, an essential step in the proton conduction mechanism.

## **5.7 CLASSIFICATION OF PROTON CONDUCTORS**

Classification of proton conductors according to preparation methods, chemical composition, structural dimensionality, mechanism of conduction etc. has been summarized in a comprehensive book on proton conductors [22]. Proton conducting materials when classified on the basis of the “range of temperature” in which they can be used in various technological applications is however most important. Proton conduction and devices employing it can be considered in three temperature ranges:

- Near ambient temperature ( $< 100$  °C)
- Medium temperature (100 – 190 °C)
- High temperature ( $> 190$  °C).

There are a huge number of proton conductors at near ambient temperature. Here, conductivity is mainly due to the presence of loosely bound water in the structure. However, conductivity in these materials is retained only up to the

temperatures where these water molecules are retained. Thus, important developments are expected for medium temperature proton conductors. Studies in the medium temperature range have established protonic conduction in  $\text{H}_3\text{O}^+$  exchanged and phosphoric acid bonded forms of known alkali ion conductors such as NASICON ( $\text{Na}_{1-x}\text{Zr}_2\text{Si}_x\text{P}_{3-x}\text{O}_{12}$ ,  $0 \leq x \leq 3$ ) and in anhydrous acid salts such as  $\text{CsHSO}_4$ .

Proton conductors have also been classified as “framework hydrates” and “particle hydrates” [23].

**Framework hydrates:** are strongly bonded covalent structures where conduction ions reside in tunnels or cavities and the conduction may occur in the interior or throughout the entire particle. Their structure may be layered (two dimensional) or three dimensional. Proton conductivity in these compounds depend on the presence of water or other proton carriers such as ammonia and the type of diffusion path provided for the proton by the framework structure. The conductivity is indeed that of the bulk crystal and not a surface effect.

**Particle hydrates:** The particle hydrates consist of charged particles, separated by aqueous solution, which in fact can be restricted to the first layers of water adsorbed at the surface of these granular particles. Particle hydrates have dense interiors. However, their surfaces contain hydroxyl groups, oxo groups and water molecules. The acidity of such hydrates is determined by the degree of protonation on the surface. The charge excess at the surface is balanced by the presence of protons, either as water molecules or hydroxyl groups. A particle hydrate whose surface contains an abundance of  $\text{O}^{2-}$  groups is negatively charged. Therefore, compensating  $\text{H}_3\text{O}^+$  ions are present in the interparticle water. In contrast, particle hydrates for which the surface is mainly covered by hydroxyl groups and water molecules will have an excess positive charge, compensated to  $\text{OH}^-$  groups in the interparticle water. Conductivity in particle hydrates depends upon the particle size, degree of hydration and the extent of particle ageing.

In both particle and framework hydrates the loss of all or most of the nucleophiles ( $\text{H}_2\text{O}$  and  $\text{NH}_3$ ), forces the protons to the positions on the lattice oxygen. Proton transport then takes place by hopping along lattice sites. This procedure requires a constant breaking and making of bonds with concomitant high activation energy, with decreased proton conduction.

## 5.8 APPLICATIONS OF PROTON CONDUCTORS

Discovering new proton conductors and studying the mechanism of their conduction is an area of current interest, the potential use of such compounds being in fuel cell applications, sensors, water electrolysis units and other electrochemical devices.

Proton conduction plays a key role in important processes as diverse as photosynthesis in green plants and the production of electricity in a hydrogen fuel cell. The direct application of solid-state proton conduction occurs in situations where there is a requirement to transmit hydrogen across some intervening barrier. This occurs in fuel cell technology with H<sub>2</sub>/O<sub>2</sub> cells where materials with good proton-conducting ability, but blocking to electrons and insoluble in water, would be of great value. Catalytic aspects appear in inorganic applications, where proton transport may be required on or through the solid catalyst in hydrogenation and dehydrogenation processes, while much thermal decomposition involve the loss of water, perhaps following an initial movement of protons, so that examination of proton conductivity can aid in elucidation of the process.

Interest in proton conductors has increased considerably in recent years especially because of their applications in many electrochemical devices operating either with high current densities (electrolyzer, batteries) or at low current (electrochemical sensors, memories, electro chromic devices etc.) The discovery of good solid state protonic conductors will lead to further developments in the realization of the H<sub>2</sub>/O<sub>2</sub> fuel cell, hydrogen pumps, and in general to hydrogen technologies. The applications of the proton conductors are briefly described below:

**Technological applications:** Energy conversion and signal (information) transfer in most technological applications rely on electronic conductivity, either in metals or semiconductors. Since the early days of the industrial revolution, there have always been devices, which depend on proton transport. Most conventional batteries rely on the proton conductivity of the corresponding aqueous electrolyte and at least some mixed conductivity (protonic and electronic) in the active electrode masses. So do many conventional gas sensors operating around room temperature. Even large-scale fuel cells with a power output in the MW range benefit from the high proton conductivity of phosphoric acid. Besides these traditional applications, the progressive availability of solid proton-conducting materials stimulated the utilization

of proton conduction in a variety of devices for energy conversion, chemical sensing, the production of chemicals, and electrochromic displays.

***Fuel and electrolysis cells:*** Stimulated by the aggravation of the legislative pollution control in most industrialized nations, activities in the development of batteries and fuel cells, i.e., devices directly converting chemical into electrical energy, have increased. It is the aim to avoid combustion processes with their inherent limits of thermodynamic efficiencies and their production of hazardous gases such as NO<sub>x</sub> and CO.

***Electrochemical sensors:*** Many sensors relying on acid/base reactions have a proton conductor as a separator. In close analogy to the well-known oxygen probe based on yttria-stabilized zirconia, a potentiometric sensor for measuring hydrogen activities in aluminum melts based on indium-doped CaZrO<sub>3</sub> has been developed [24] and commercialized.

Sensors based on proton-conducting oxides have been suggested for the sensing of humidity [25, 26], of alkanes (methane, ethane, propane) [27], for alcohols (ethanol) [28] and even of CO<sub>2</sub> [29]. They have been reviewed by Iwahara [30].

Sensors for CO, NH<sub>3</sub>, O<sub>2</sub>, H<sub>2</sub>O<sub>2</sub>, and even glucose, using hydrated antimony oxide as electrolyte, have been reviewed by Miura and Yamazoe [31]. The coating of electrodes by hydrated proton-conducting polymers is also very popular. These have been used in sensors utilizing enzymes for the detection of cholesterol [32] or oxygen [33]. Sensors based on “pellicular” zirconium phosphate have been tested for the detection of CO [34], O<sub>2</sub> [35], and H<sub>2</sub> [36]. Sensors based on acid zirconium phosphates and phosphonates have been reviewed by Alberti, Casciola, and Palombari [37].

***Electrochemical reactors:*** In near future, it is proposed to use proton-conducting separators in “electrochemical pump”, hydrogen in or out of a reactor, thus influencing or even controlling hydrogenation and dehydrogenation reactions [38].

***Electrochromic devices:*** Recently, solid materials with high proton conductivity have attracted much attention for application in a variety of electrochemical devices. There have been extensive activities in the development of electrochromic devices (displays, windows, mirrors) based on solid fast ionic conductors also including proton conductors, which have recently been reviewed by Bohnke [22].

## 5.9 FUEL CELLS - NOVEL CONCEPT FOR POWER GENERATION

**Fuel cell perspective:** No other energy generating technology carries the combination of benefits that fuel cells offer. A fuel cell running on pure hydrogen is a zero emission power source. Fuel cells use natural gas or hydrocarbons as a hydrogen feedstock, produce less emission, more efficient than conventional power plants, and also reduce noise pollution. Different type of fuel cells and their applications and environmental impact are shown in **Table 5.1** and **5.2**.

From **Table 5.1** and **5.2**, it is clear that Proton Exchange Membrane Fuel Cells (PEMFC) is one of the most promising clean energy generating technology. Current technology for PEMFC's is limited by its inability to operate at high temperatures (> 100 °C) [21].

**Table 5.1** *Types of fuel cell and its applications*

Fuel Cell	Electrolyte, operating temperature, efficiency	System Output	Applications
Proton exchange Membrane FC (PEMFC)	Nafion (proton conductor), 60 - 100°C, 40 - 50 %	< 1 - 250 kW	Portable Stationary Automotive
Alkaline FC (AFC)	Potassium hydroxide, 100 - 250°C, 60 %	10 - 100 kW	Space
Phosphoric Acid FC (PAFC)	Phosphoric Acid, 150 - 200°C, 32-38 %	50 kW-1 MW	Large Stationary
Molten Carbonate FC (MCFC)	Alkali carbonates, 600 - 700 °C, 45-47 %	250 kW-1 MW	Power plants
Solid Oxide FC (SOFC)	Yittria stabilized zirconia, 650-1000 °C, 35- 43 %	5 kW - 3 MW	Small and Large stationary

**Table 5.2** *Environmental overview*

Power Generator	NO <sub>x</sub> emissions (g/MWh)	CO <sub>x</sub> emissions (kg/MWh)	Output
Fuel Cells	1.36	336	Electricity and Heat
Grid Power	500	600	Electricity
Diesel	170	824	Electricity
NG heater	230	240	Heat

**How fuel cells (PEMFC) work:**The core of the fuel cell consists of a membrane electrode assembly (MEA), which is placed between two flow-field plates. The MEA

consists of two electrodes, the anode and the cathode, which are each coated on one side with a thin catalyst layer and separated by a proton exchange membrane (PEM). The flow-field plates direct hydrogen to the anode and oxygen (from air) to the cathode. When hydrogen reaches the catalyst layer, it separates into protons (hydrogen ions) and electrons. The free electrons, produced at the anode, are conducted in the form of a usable electric current through the external circuit. At the cathode, oxygen from the air, electrons from the external circuit and protons combine to form water and heat. A schematic diagram of PEMFC is presented in **Figure 5.6**.

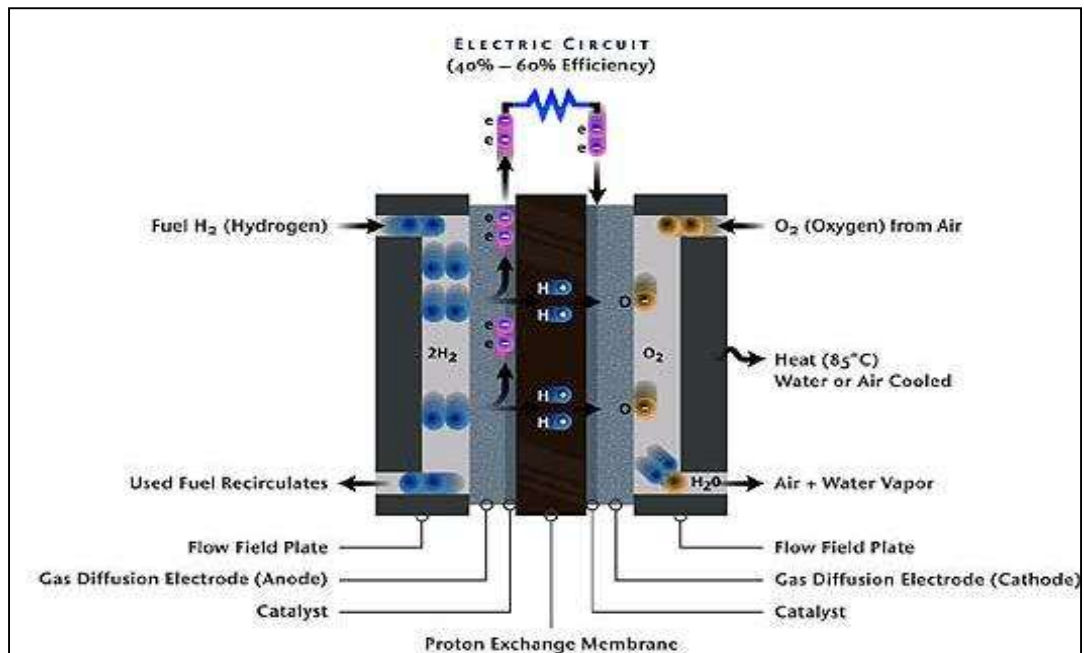
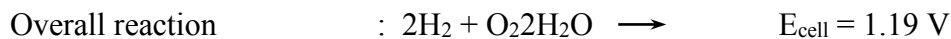
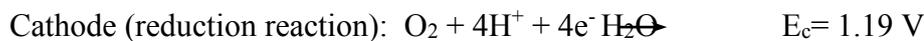
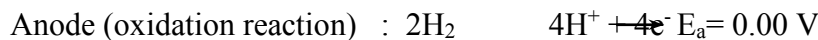


**Figure 5.6** A schematic diagram of PEMFC



### 5.10 CURRENT STATUS

In PEMFC, Proton exchange membranes (PEM) is the heart of the fuel cell. Nafion, a perfluorosulfonic acid polymer, is the most widely used proton conductor in PEMFC. However, the high cost of Nafion and the environmental hazards associated with its disposal have prompted research for low-cost non-perfluorinated ionomer membranes, which are more environment friendly. Further, Nafion must be well hydrated to obtain optimum performance because its proton conduction relies on

dissociation of protons from ion exchange groups in presence of water [21, 39]. Thus, PEMFC is usually operated at below 100 °C to maintain sufficient hydration of Nafion. Fuel cells operating at medium temperatures (120 - 160 °C), is also limited by unavailability of materials that exhibit good proton conductivity at elevated temperatures. The achievement of such an aim is challenging and it needs the development of proton conducting materials that are able to work in dry or low humidity environments.

The demand for new power sources and environmental monitoring, determine the need for new materials possessing high proton conductivity. The key area of research in recent years is high temperature membranes or the so called solid acid membranes with high proton conductivity. In recent years, only a few new materials with high proton conductivity have been obtained [40]. This necessitates the modification of known materials to improve their conducting properties.

Protonic conduction is present in a wide range of systems such as clays, glass, inorganic ion exchangers in the hydrogen form, heteropoly acids etc. The typical solid-state protonic conductors developed a couple of decades ago, were mainly acidic or hydrous inorganic compounds. Later, entirely different classes of materials gained increasing interest as proton conductors: polymers, oxide ceramics, intercalation compounds, etc. Protonic conduction is also present in anhydrous acid salts such as CsHSO<sub>4</sub>. A brief overview of the various materials used as solid state proton conductors and methods of enhancement in proton conductivity in these materials has been reported by Hogarth et al [21], with a special focus towards enhancement of proton conductivity by surface functionalization, surface area modification and adopting new synthetic routes.

A summary of some of the materials exhibiting promising results are shown in **Table 5.3**.

**Table 5.3** Summary of the various proton conducting materials

Compounds	$\sigma$ (Scm <sup>-1</sup> )	Conditions
<b>Composites</b>		
Nafion/ $\alpha$ -ZrP	0.10	100 °C, 100% RH
SPEEK/ $\alpha$ -ZrP	0.01	25 °C, 100 % RH
Imidazole/Nafion (Transverse)	0.10	160 °C, 100% RH
<b>Zirconium</b>		
$\alpha$ -Zr(O <sub>3</sub> POH) <sub>2</sub> ·H <sub>2</sub> O	10 <sup>-5</sup> to 10 <sup>-6</sup>	20 °C, 90 % RH 180 °C, 00 % RH
$\alpha$ -Zr(O <sub>3</sub> POH) <sub>2</sub>	1.0 × 10 <sup>-7</sup>	20 °C, 90 % RH
Pellicular $\alpha$ -Zr(O <sub>3</sub> POH) <sub>2</sub> ·nH <sub>2</sub> O	1.0 × 10 <sup>-4</sup>	20 °C, 90 % RH
$\alpha$ -Zr(O <sub>3</sub> PCH <sub>2</sub> OH) <sub>1.27</sub> (O <sub>3</sub> PC <sub>6</sub> H <sub>4</sub> SO <sub>3</sub> H) <sub>0.73</sub> ·nH <sub>2</sub> O	1.6 × 10 <sup>-2</sup> 8.0 × 10 <sup>-3</sup>	20 °C, 90 % RH 100 °C, 60 % RH
$\alpha$ -Zr(O <sub>3</sub> PCH <sub>2</sub> OH) <sub>1.15</sub> (O <sub>3</sub> PC <sub>6</sub> H <sub>4</sub> SO <sub>3</sub> H) <sub>0.85</sub>	1.2 × 10 <sup>-4</sup>	180 °C, 00 % RH
$\alpha$ -Zr(O <sub>3</sub> PC <sub>6</sub> H <sub>4</sub> SO <sub>3</sub> H) <sub>2.3</sub> ·6H <sub>2</sub> O	2.1 × 10 <sup>-2</sup>	105 °C, 85 % RH
$\gamma$ -Zr(PO <sub>4</sub> )(H <sub>2</sub> PO <sub>4</sub> )·2H <sub>2</sub> O	2.0 × 10 <sup>-5</sup>	20 °C, 90 % RH
$\gamma$ -Zr(PO <sub>4</sub> )(H <sub>2</sub> PO <sub>4</sub> ) <sub>0.54</sub> (HO <sub>3</sub> PC <sub>6</sub> H <sub>4</sub> SO <sub>3</sub> H) <sub>0.46</sub> ·nH <sub>2</sub> O	1.0 × 10 <sup>-2</sup>	20 °C, 90 % RH
Zirconium phosphate (Sol-gel)	3.0 × 10 <sup>-2</sup>	20 °C, 50 % RH
Zirconium phosphate pyrophosphate	1.3 × 10 <sup>-3</sup> 2.0 × 10 <sup>-6</sup>	20 °C, 90 % RH 100 °C, 2 % RH
<b>Titanium</b>		
Ti(HPO <sub>4</sub> ) <sub>0.25</sub> (O <sub>3</sub> PC <sub>6</sub> H <sub>5</sub> ) <sub>0.12</sub> (O <sub>3</sub> PC <sub>6</sub> H <sub>4</sub> SO <sub>3</sub> H) <sub>1.63</sub>	1.3 × 10 <sup>-1</sup>	5 °C, 85 % RH
<b>Cesium</b>		
$\beta$ -Cs(HSO <sub>4</sub> ) <sub>2</sub> (H <sub>2</sub> (PS)O <sub>4</sub> )	3.0 × 10 <sup>-5</sup> 1.6 × 10 <sup>-2</sup>	90 °C 200 °C
$\alpha$ -Cs(HSO <sub>4</sub> ) <sub>2</sub> (H <sub>2</sub> (PO) <sub>4</sub> )	2.5 × 10 <sup>-3</sup>	40 °C
<b>Cerium</b>		
Ce(HPO <sub>4</sub> ) <sub>2</sub>	7 × 10 <sup>-8</sup>	180 °C
Ce <sub>0.98</sub> Sr <sub>0.02</sub> PO <sub>4-<math>\delta</math></sub>	3.48 × 10 <sup>-3</sup>	600 °C
Ce <sub>0.7</sub> Mg <sub>0.3</sub> P <sub>2</sub> O <sub>7</sub>	1.5 × 10 <sup>-2</sup>	180 °C
Ce <sub>0.8</sub> Mg <sub>0.2</sub> P <sub>2</sub> O <sub>7</sub>	1.5 × 10 <sup>-2</sup>	180 °C
Ce <sub>0.9</sub> Mg <sub>0.1</sub> P <sub>2</sub> O <sub>7</sub>	4.0 × 10 <sup>-2</sup>	200 °C
Gd doped Ce <sub>2</sub> P <sub>2</sub> O <sub>7</sub>	3.98 × 10 <sup>-5</sup> 3.16 × 10 <sup>-5</sup> 2.56 × 10 <sup>-5</sup>	Dry H <sub>2</sub> O D <sub>2</sub> O
Cerium sulfonyl phosphate (CeSPP)/poly (2,5-benzimidazole) (ABPBI) composite membrane	1.4 × 10 <sup>-1</sup> 0.9 × 10 <sup>-1</sup>	180 °C, 38 % RH 180 °C, 18 % RH
<b>Thorium</b>		
Polypyrrole thorium phosphate (40% pyrrole concentration)	5.16 × 10 <sup>-4</sup>	Ambient temp.
<b>Others</b>		
Fullerene	7 × 10 <sup>-7</sup>	20 °C

## 5.11 LITRETURE SURVEY IN THE CURRENT AREA OF STUDY

### *TMA salts as Proton Conductors*

The mechanism of diffusion and proton transport in various TMA salts, zirconium phosphate, titanium phosphate, tin phosphate, tantalum phosphate, uranyl phosphate have been studied in detail by various workers [41-44]. Amongst the various TMA salts, zirconium phosphate ( $\alpha$ -ZrP) and titanium phosphate ( $\alpha$ -TiP), have been extensively studied as proton conductors [45,46].

Zirconium phosphate (ZrP) behaves as protonic conductor because of the presence of structural hydroxyl groups giving rise to surface  $H^+$  sites. Zirconium phosphate occurs in two forms,  $\alpha$ -ZrP and  $\gamma$ -ZrP. The structure of  $\alpha$ -ZrP lends itself best to proton transport because it has a pendant  $-OH$  group which extends into the interlayer region and forms a hydrogen bonded network with water. The  $\gamma$ -ZrP does have the advantage of having an extra water molecule per formula unit and is more acidic than the  $\alpha$ -ZrP [47]. In  $\alpha$ -ZrP, proton conductivity measurements was first demonstrated by DC measurements performed at room temperature with platinum electrodes in argon or hydrogen atmosphere [48]. It was observed that the conductivity in hydrogen atmosphere (where the electrodes are non blocking to protons and electrons) is more than two orders of magnitude higher than that measured in argon (where the electrodes are non blocking to electrons and blocking to protons).

Clearfield has observed charge balancing protons ( $H^+$ ) bonded to oxygen, adjacent to interlayer region in  $\alpha$ -ZrP lamellar microanions  $[Zr_n(PO)_4^{2n}]^{2n-}$ . These protons are responsible for the proton conductivity in ZrP [49]. When these  $-OH$  groups are hydrated, the protons can move easily on the surface, thus accounting for their conductivities, which depend strongly on relative humidity, the surface area and the degree of crystallinity [50]. In anhydrous conditions, the distance among the adjacent surface  $-OH$  groups is too high to permit direct jumps between one site to another. At room temperature and different relative humidities, the conductivity of the monohydrated material is dominated by surface transport and affected to a great extent by surface hydration [51, 52]. Between 100-300 °C, the conductivity of the anhydrous material is a bulk property, the activation energy depending on the inter layer distance [17, 18, 53].

Alberti and coworkers have studied proton conductivity of ZrP, and they found that inspite of the very high concentration of acid groups in these materials, the bulk contribution to the conductivity was negligible. The main part of the measured conductivity is related to the surface P-OH groups and its value strongly depends on the surface area of the micro crystals. Alberti et al were able to show that the surface conducts protons thousand times faster than the interior [54]. The very low bulk conductivity at room temperature could be due to the lack of orientation and polarization of the P-OH groups present in the interlayer region of  $\alpha$ -ZrP. On the other hand P-OH groups present on the surface have much more freedom to rotate than the internal ones and that proton transport is assisted by water molecules forming a bridge between the acid groups [55]. Isoconductance measurements also indicate that the conductivity varies linearly with the number of surface phosphate groups [56]. In addition, conductivity in  $\alpha$ -ZrP is highly dependant on the hydration, varying by two orders of magnitude as the relative humidity (RH) is increased from 5 to 90 % [51]. Alberti and coworkers have also shown that the proton conductivity is strongly influenced by the species present in the interlayer region [56]. An early investigation on ZrP with varying degrees of crystallinity shows that the conductivity decreases considerably with increasing degree of crystallinity [54, 57, 58]. Moreover, it has been found that the conductivity of  $\alpha$ -ZrP pellets, depends on the size of particles [59, 60] and density of the pellets [51].

Alberti and coworkers have also made some efforts to improve the proton conduction properties of  $\alpha$ -ZrP. A modified ZrP (sonicated-lipophilized $\alpha$ -ZrP) was prepared by putting the colloidal dispersion under sonication, followed by lipophilization of the  $\alpha$ -ZrP [61]. Due to the larger surface area and the preferred orientation, the conductivities of pellicular $\alpha$ -ZrP and sonicated-lipophilized $\alpha$ -ZrP were found to be one to two orders of magnitude higher than that of microcrystalline $\alpha$ -ZrP.

Alberti and coworkers [62, 63] have investigated the proton conductivity of titanium(IV) phosphates (TiP) and found that the conductivity is comparable to that of ZrP. As in case of  $\alpha$ -ZrP, here also the conductivity is essentially due to hydrated cations present on the surface of the microcrystals. MesoporousTiPs synthesized by the sol-gel route using surfactant templates shows good conductance compared to ZrP [63]. Hogarth et al have also studied the proton transport properties of TiP synthesized

by sol-gel method, and reported conductance of the order  $0.0044 \text{ S}\cdot\text{cm}^{-1}$  and  $0.0019 \text{ S}\cdot\text{cm}^{-1}$  (100 % RH, 100 °C) for amorphous and crystalline phases respectively [46].

Casciola and Constantino et al [64] have reported *ac* conductivity of CP in hydrogen form. Dah-Shyang Tsai et al [65] have reported the crystal structure and proton conductivity of cerium pyrophosphate to explore its potential electrolyte applications for intermediate temperature fuel cell. Onoda et al have [66] reported synthesis and electrical conductivity of bulk tetravalent cerium pyrophosphate. Nicole et al have [67] reported structure and electronic properties of cerium orthophosphate. EG Moaral et al [68] have reported impedance analysis of Sr-substituted  $\text{CePO}_4$  with mixed protonic and p-type electronic conduction. Zhongfang Li et al [69] have reported synthesis and characteristics of proton-conducting membranes based on cerium sulfophenyl phosphate and poly (2,5-benzimidazole). Khan et al have [70] reported electrical conductivity study of an organic-inorganic composite cation exchanger: polypyrrole-TP.

***Work carried out in our laboratory***

From our laboratory, proton transport properties of TMA salts - tungstates and phosphates of  $\text{Sn}^{4+}$ ,  $\text{Ti}^{4+}$  and  $\text{Zr}^{4+}$  have been reported, where it is observed that specific conductivity decreases with increasing temperature and the mechanism of conduction is suggested to be of Grotthuss type [71, 72].

Proton conduction behaviour of hybrid materials have also been studied with an aim to examine enhancement of proton conductivity by surface modification. Hybrid materials have been prepared by anchoring organic moieties, ortho-chlorophenol and para-chlorophenol onto tungstates of  $\text{Sn}^{4+}$ ,  $\text{Ti}^{4+}$  and  $\text{Zr}^{4+}$  [73] as well as tiron onto zirconium molybdate [74]. The mechanism of conduction is suggested to be Grotthuss type. Further, low values of energy of activation suggest the ease of conduction. Proton transport properties of zirconium (IV) phosphonates show enhanced conductance compared to ZrP [75].

A literature survey as well as work conducted in our laboratory shows that not much work has been done on the proton transport properties of amorphous CP and TP.

***In the present study CP, TP,  $\text{CP}_M$  and  $\text{TP}_M$  have been explored as solid state proton conductors.***

## 5.12 EXPERIMENTAL

**Materials and Methods:** The synthesis and characterization of CP, TP, CP<sub>M</sub> and TP<sub>M</sub> has been described in **Chapter II, Section 2.3 and 2.4**.

**Experimental set up:** The proton conductivity of the materials were measured using pellets of 10 mm diameter and 1.5 - 2 mm thickness which were prepared by pressing ~ 300 mg of material at 40 KN/cm<sup>2</sup>. The two opposite flat surfaces of the pellets were coated with conducting silver paste to ensure good electrical contacts. Specific conductivity was measured in the temperature range 30 °C - 120 °C at 10 °C intervals, using Solartron impedance analyzer (SI 1260) over a frequency range 1 Hz - 32 MHz at a signal level below 1 V, interfaced to a computer for data collection.

**Specific Conductivity Measurements:** Specific conductivity is measured using impedance analyzer. In this technique, a small amplitude AC signal is applied to the system being studied, and amplitude and phase of the resulting current measured. The amplitude of the AC signal is chosen to be small enough to assume a linear response of the material. Usually the impedance, the ratio of the applied voltage to the resulting current, is computed and analyzed. The electrical impedance of an electrochemical cell can be measured either directly with an impedance analyzer, or with a combination of a frequency response analyzer (FRA) and an electrochemical interface (ECI). The ECI is a high bandwidth potentiostat that provides the DC cell bias voltage or current, and a small sinusoidal AC signal (typically a few millivolts) from the FRA, is superimposed. The AC response from the cell over a range of applied frequencies is analyzed by the FRA and the impedance calculated.

An impedance spectrum is a plot of the in phase (imaginary impedance) components of the vector impedance ( $z$ ) as a function of the frequency of an ac electrical stimulus. Each point generated in complex plane corresponds to a measurement at a different frequency. This is also known as Nyquist plot or colecoleplot or complex impedance plot [76].

The impedance diagrams measured on a sintered compact are shown in **Figure 5.7**. They can be divided into three different contributions (**Figure 5.7**). At low frequency a straight line is observed, characteristic of the sample-electrode interface. At high frequency, the bulk response of the sample gives rise to a semicircle. At intermediate frequencies a third contribution, that appears for the low temperatures

and/or for the low relative humidity only, can be attributed to a grain boundary contribution, in agreement with similar works [77].

The complex impedance plot presented in **Figure 5.8**, consists of a single depressed semicircle. The sample resistance ( $R$ ) was measured by extrapolation of the high frequency arc crossing to the  $Z'$  (real) axis. The proton conductivity was measured using the equation,  $\sigma = l/RA$ , where  $\sigma$  is the conductivity ( $S \cdot cm^{-1}$ ),  $l$  is the thickness of the sample (cm) and  $A$  is the electrode area ( $cm^2$ ).

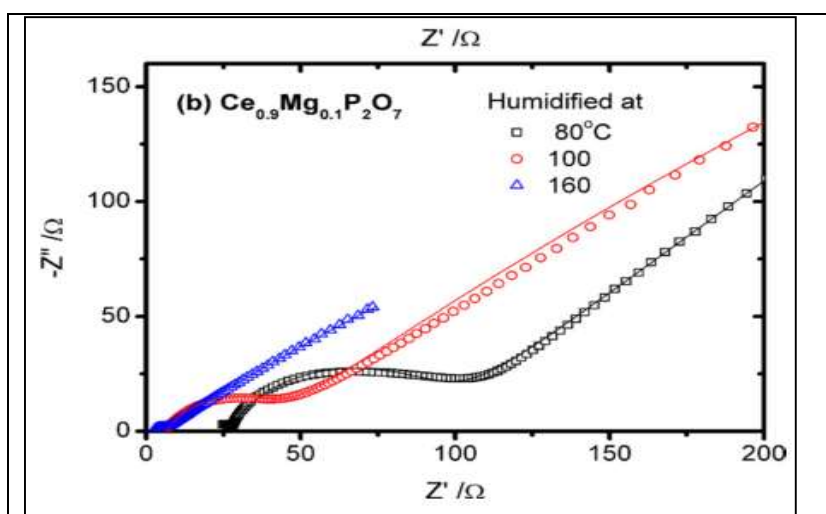


**Figure 5.7** Complex impedance plot [77]

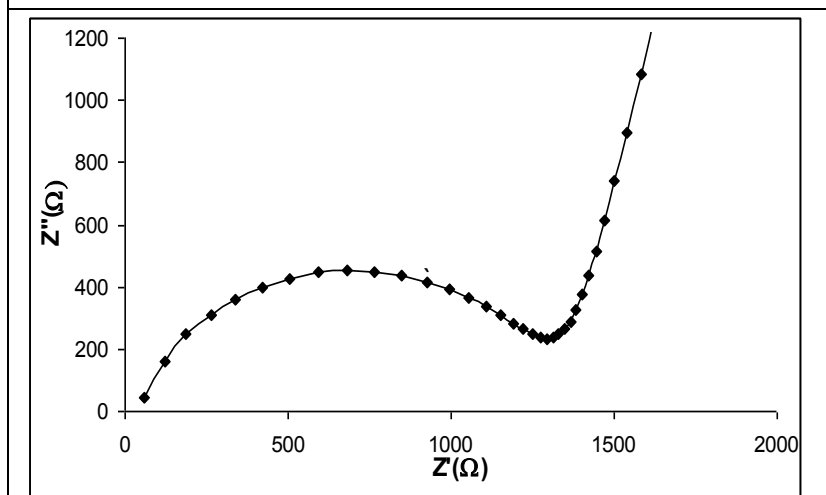


**Figure 5.8** Complex impedance plot

Ionic conductivities of solid electrolytes display Arrhenius-type temperature dependencies i.e. a linear variation of  $\ln(\sigma T)$  with  $1/T$ . Hence, it is possible to calculate the values of the activation energy  $E_a$  from the plot of  $\ln(\sigma T)$  vs.  $1/T$ . The

values of the activation energy  $E_a$  for each of the samples was calculated using the Arrhenius equation  $\sigma = \sigma_0 \exp(-E_a/kT)$ , where  $k$  is Boltzmann's constant and  $T$  is temperature.

In all cases, since the impedance plots of the materials consist of single depressed semicircle, the pellet conductivity was calculated by arc extrapolation to the real axis, taking into account the geometrical sizes of the pellets.

### **5.13 RESULTS AND DISCUSSION**

The results of specific conductance ( $\sigma$ ) for CP, CP<sub>M</sub>, TP and TP<sub>M</sub> have been presented in **Table 5.4**. The complex impedance plots (at 30°C) and Arrhenius plots ( $\log \sigma T$  versus  $1/T$ ) have been presented in **Figures 5.9(a-d) and 5.10(a-d)**.

For all the materials, it is observed that specific conductivity decreases with increasing temperature (**Table 5.4**). Similar trend in TMA salts have been observed earlier by us [71-73]. This is attributed to the loss of water of hydration as well as condensation of structural hydroxyl groups with increasing temperature. This fact is also supported by study of the effect of heating on CEC, where CEC values decrease as calcination temperature increases. This suggests the mechanism of transportation to be of Grotthuss type [45], where the conductivity depends on the ability of the water located on the surface to rotate and participate. Further, the results are also in agreement with the suggestion that protons are not able to diffuse along an anhydrous surface, where the spaces between –OH groups are very large [78]. Besides, the fact that the loss of protons resulting from hydroxyl condensation causes considerable decrease in conductivity also indicates that the conduction is protonic. These factors reveal the importance of water in the conduction mechanism.

The order of specific conductance at 30°C (**Table 5.4**) is found to be CP<sub>M</sub> ( $3.17 \times 10^{-6} \text{S}\cdot\text{cm}^{-1}$ ) > CP ( $4.57 \times 10^{-7} \text{S}\cdot\text{cm}^{-1}$ ) > TP<sub>M</sub> ( $2.76 \times 10^{-7} \text{S}\cdot\text{cm}^{-1}$ ) > TP ( $3.33 \times 10^{-8} \text{S}\cdot\text{cm}^{-1}$ ). This trend is also in keeping with the CEC values in parenthesis, CP<sub>M</sub> (2.90) > CP (2.45) > TP<sub>M</sub> (2.41) > TP (1.48). Higher CEC as well as surface acidity values (**Chapter II, Table 2.6**) indicate more exchangeable protons ( $\text{H}^+$  of structural –OH group in present case) and hence more conducting protons (**Table 5.4**).

In the present study, since the phosphate anion is common for CP and TP, the proton conductivity of the phosphates should bear a correlation with the acidity of the cations. Acidity of a cation is related to ion size and charge. The ionic radius for

Ce<sup>4+</sup> is 1.05 Å (180pm) and Th<sup>4+</sup> is 1.08 Å (185pm) [79]. Ce<sup>4+</sup> with a smaller ionic radii and therefore a high charge density, exhibits higher proton conductivity. The specific conductivity of CP and TP is lower compared to amorphous zirconium(IV) phosphate (ZrP) { $2.3 \times 10^{-6} \text{S}\cdot\text{cm}^{-1}$ } [76], titanium (IV) phosphate (TiP) { $4.03 \times 10^{-5} \text{Scm}^{-1}$ } [75] and tin (IV) phosphate (SnP) { $7.6 \times 10^{-6} \text{S}\cdot\text{cm}^{-1}$ } [75]. However, the specific conductivity value of CP<sub>M</sub> is comparable to ZrP.

$E_a$  values depend on several factors such as high density of mobile ions, the availability of vacant sites, good connectivity among the sites, complexity in structure/steric effect and acidity of the metal ion. Stenina et al [43] have attributed strong H-bonding to higher  $E_a$  values. However, observed  $E_a$  is a result from the contribution of the above-mentioned factors. Depending on the predominant factor, the  $E_a$  values vary in each case.

In **Figures 5.9(c-d) and 5.10(c-d)** (Arrhenius plots,  $\text{Log}(\sigma T)$  versus  $1000/T$ ) linearity is observed in the temperature range 90–120°C for all the materials (**Table 5.4**). The energy of activation ( $E_a$ ) (in parenthesis) has been found to be CP<sub>M</sub> (1.15), CP (2.10), TP<sub>M</sub> (4.86) and TP (7.30) kcal·mol<sup>-1</sup>.  $E_a$  values, follow the order TP > TP<sub>M</sub> > CP > CP<sub>M</sub> in the temperature range 90-120 °C, while, specific conductance values follow the order CP<sub>M</sub> > CP > TP<sub>M</sub> > TP. A lower value of  $E_a$  indicates ease of conduction and also suggests the mechanism to be Grotthuss type where  $E_a$  entirely depends on reorientation of water molecules on the surface. In the present study trend in  $E_a$  and specific conductivity ( $\sigma$ ) are supportive to each other.

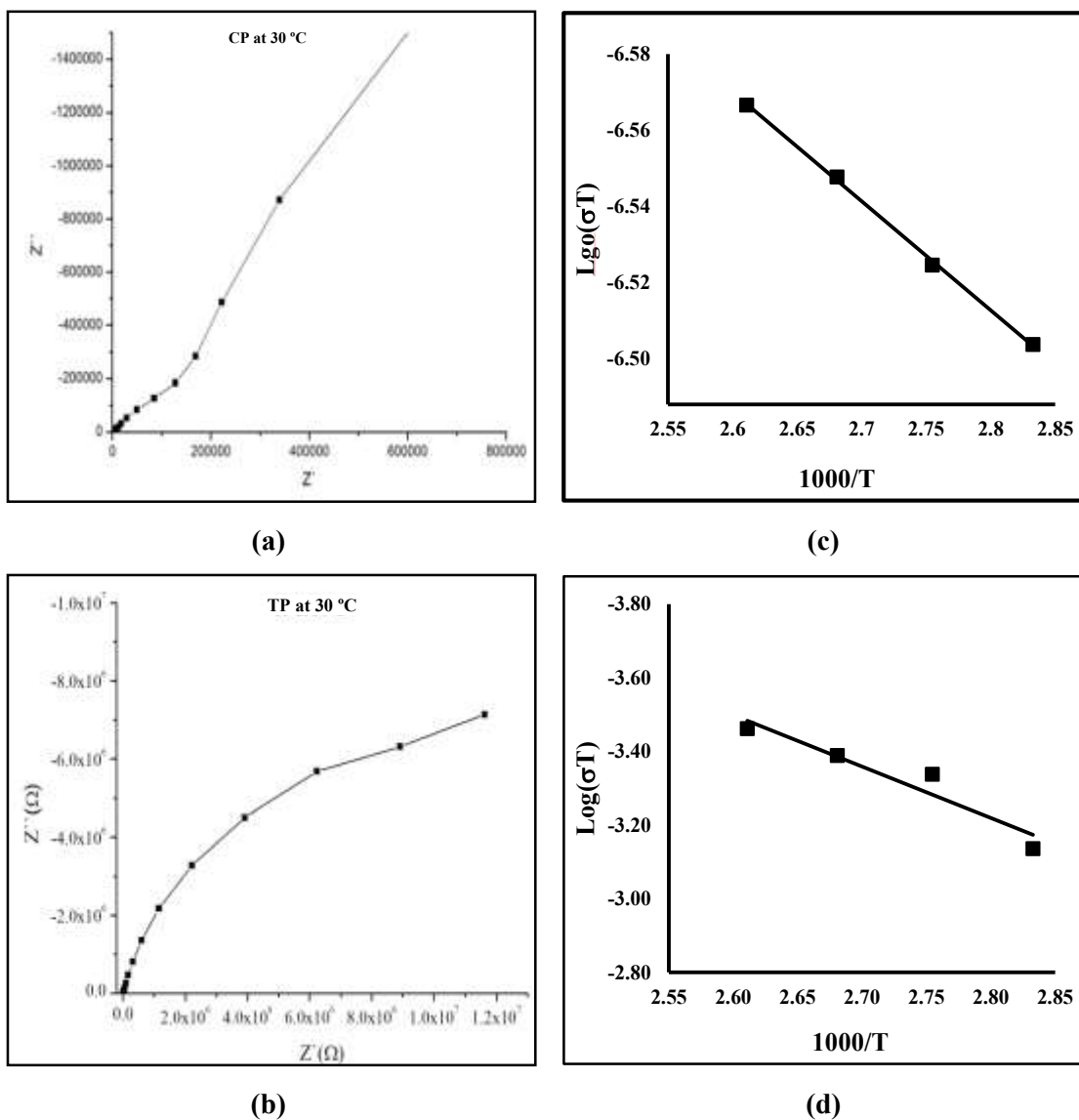


**Figure 5.9** Complex impedance plots (at 30 °C) for (a) CP, (b) TP and Arrhenius plots (temperature range 90-120 °C) for (c) CP and (d) TP

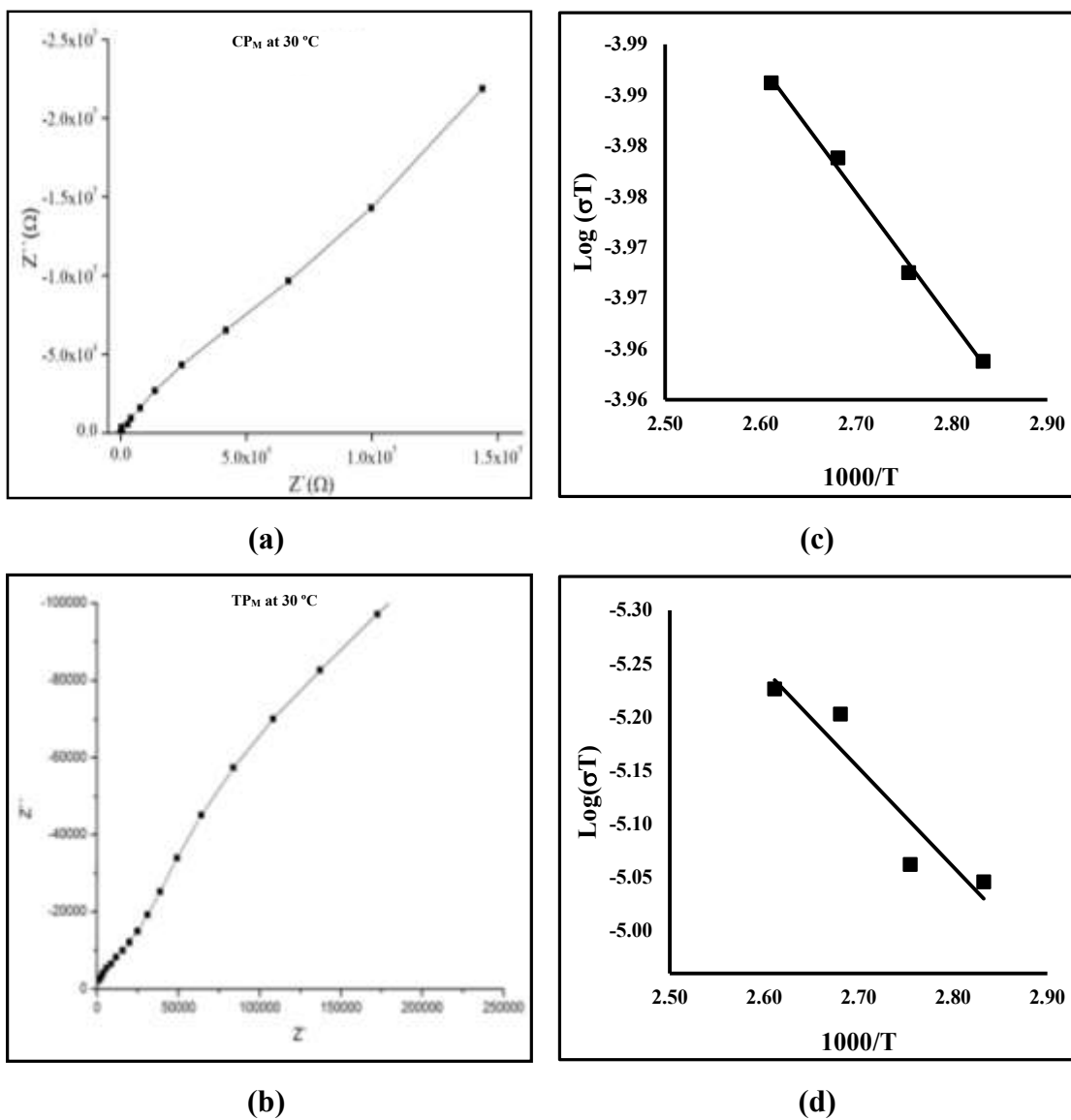


**Figure 5.10** Complex impedance plots (at 30 °C) for (a) CP<sub>M</sub>, (b) TP<sub>M</sub> and Arrhenius plots (temperature range 90-120 °C) for (c) CP<sub>M</sub> and (d) TP<sub>M</sub>

**Table 5.4** Specific conductance  $\sigma$  ( $S \cdot cm^{-1}$ ) of CP, TP, CP<sub>M</sub> and TP<sub>M</sub> at various temperatures

Temperature (°C)	$\sigma$ CP	$\sigma$ CP <sub>M</sub>	$\sigma$ TP	$\sigma$ TP <sub>M</sub>
30	$4.57 \times 10^{-7}$	$3.17 \times 10^{-6}$	$3.33 \times 10^{-8}$	$2.76 \times 10^{-7}$
40	$4.44 \times 10^{-7}$	$3.11 \times 10^{-6}$	$3.17 \times 10^{-8}$	$2.21 \times 10^{-7}$
50	$4.18 \times 10^{-7}$	$3.02 \times 10^{-6}$	$3.04 \times 10^{-8}$	$2.19 \times 10^{-7}$
60	$3.30 \times 10^{-7}$	$2.62 \times 10^{-6}$	$2.86 \times 10^{-8}$	$2.19 \times 10^{-7}$
70	$3.28 \times 10^{-7}$	$2.02 \times 10^{-6}$	$2.71 \times 10^{-8}$	$2.15 \times 10^{-7}$
80	$3.11 \times 10^{-7}$	$1.94 \times 10^{-6}$	$2.55 \times 10^{-8}$	$2.07 \times 10^{-7}$
90	$2.97 \times 10^{-7}$	$1.74 \times 10^{-6}$	$2.39 \times 10^{-8}$	$1.26 \times 10^{-7}$
100	$2.81 \times 10^{-7}$	$1.73 \times 10^{-6}$	$1.68 \times 10^{-8}$	$1.10 \times 10^{-7}$
110	$2.70 \times 10^{-7}$	$1.52 \times 10^{-6}$	$1.55 \times 10^{-8}$	$9.02 \times 10^{-8}$
120	$2.28 \times 10^{-7}$	$1.30 \times 10^{-6}$	$1.16 \times 10^{-8}$	$8.21 \times 10^{-8}$
<b>E<sub>a</sub></b> <b>(kcal/mol)</b>	2.10	1.15	7.30	4.86
<b>CEC</b> <b>(meq/g)</b>	2.45	2.90	1.48	1.90
<b>Surface Acidity</b> <b>(mmol/g)</b> <b>(150 °C)</b>	0.95	1.26	0.78	0.80

## 5.14 CONCLUSIONS

TMA salts, CP and TP, exhibit good proton conductance. CP<sub>M</sub> and TP<sub>M</sub> synthesized under microwave irradiation in a much shorter reaction time exhibit higher conductance compared to CP and TP. The present study was a humble attempt to explore the proton conduction properties of amorphous CP and TP. Several studies based on synthesis of CP and TP will have to be performed, with an aim to carry out surface modifications that would offer higher CEC / surface acidity and hence proton conduction. These studies are in progress in our laboratory.

**REFERENCES**

1. Guitton J, Poinsignon C, Sanchez J, *Proton Conductors*, Colomban Ph (Ed.), Cambridge University Press, Cambridge, (1992).
2. Dunn B, Farrington G C, Fast divalent ion conduction in Ba<sup>++</sup>, Cd<sup>++</sup> and Sr<sup>++</sup>  $\beta$ -aluminas, *Mater. Res. Bull.*, **1980**, 15, 1773-1777.
3. Roth W L, Reidinger F, LaPlaca A, *Superionic Conductor Colloquiu*, Mohan G D, Roth W L (Eds.), Schenectady, **1976**, 223.
4. Reau J M, Portier J, *Solid Electrolytes Fluorine Ion Conductors*, Hagenmuller P, van Gool W (Eds.), Academic Press, **1978**, Chap. 19.
5. Cotton F A, Wilkinson, *Inorganic Chemistry*, 2<sup>nd</sup>Edn., Interscience, **1966**, 894, 1040.
6. Kudo T, Flueki K, *Solid State Ionics*, VCH Publishers, New York, **1990**, Chap. 6.
7. van Grotthuss C J T, Sur la decomposition de leau et des corps quelletient en dissolution a laide de lelectricitegalvanique, *Ann. Chim.*, **1806**, 58, 54-73.
8. Chandra S, Singh N, Hashmi N A, *Proc. Indian Natn. Acad.*, **1986**, 52, 338.
9. Kreuer K D, On the development of proton conducting polymer membranes for hydrogen and methanol fuel cells, *J Membr. Sci.*, **2001**, 185, 29-39.
10. Kreuer K D, On the complexity of proton conduction phenomena, *Solid State Ionics*, **2000**, (136-137), 149-160.
11. Boysen D A, Uda T, Chisholm C R, Haile S M, High-performance solid acid fuel cells through humidity stabilization, *Science*, **2004**, 303, 68-70.
12. Haile S M, Boysen D A, Chisholm C R, Merle R B, Solid acids as fuel cell electrolytes, *Nature*, **2001**, 410, 910-913.
13. J. M. Troup, A. Clearfield, Mechanism of ion exchange in zirconium phosphates. 20. Refinement of the crystal structure of  $\alpha$ -zirconium phosphate, *Inorg. Chem.*, **1977**, 16, 3311-3314.
14. Albertson J, Oskarson A, Tellgren R, Thomas J O, Inorganic ion exchangers. 10. A neutron powder diffraction study of the hydrogen bond geometry in .alpha.-zirconium bis(monohydrogen orthophosphate) monohydrate. A model for the ion exchange, *J Phy. Chem.*, **1977**, 81, 1574-1580.

15. Alberti G, Casciola M, Constantino U, Peraio A, Rega T, Proton-conducting solid dispersions of silica and zirconium phosphate pyrophosphate, *J Mater Chem.*, **1995**, 5, 1809-1812.
16. Alberti G, Casciola M, Layered metal<sup>IV</sup> phosphonates, a large class of inorgano-organic proton conductors, *Solid State Ionics*, **1997**, 97, 177-186.
17. Alberti G, Casciola M, Constantino U, Leonardi M, ac conductivity of anhydrous pellicular zirconium phosphate in hydrogen form, *Solid State Ionics*, **1984**, 14, 289-295.
18. Clearfield A, Jerus P, Ionic conductivity of anhydrous zirconium bis(monohydrogen orthophosphate) and its sodium ion forms, *Solid State Ionics*, **1982**, 6(1), 79-83.
19. Tuckerman M, Laasonen K, Sprik M, Parrinello M, *Ab initio* molecular dynamics simulation of the solvation and transport of hydronium and hydroxyl ions in water, *J Chem. Phys.*, **1995**, 103, 150.
20. Tuckerman M, Marx D, Klein M, Parrinello M, On the quantum nature of the shared proton in hydrogen bonds, *Science*, **1997**, 275, 817-819.
21. Hogarth W H J, Diniz da Costa J C, Lu(Max) G Q, Solid acid membranes for high temperature (140° C) proton exchange membrane fuel cells, *J Power Sources*, **2005**, 142, 223-237.
22. Ikava H, *Proton Conductors*, ColombanPh (Ed.), Cambridge University Press, Cambridge, **1992**, 551.
23. Clearfield A, Structural concepts in inorganic proton conductors, *Solid State Ionics*, **1991**, 46, 35-43.
24. Yajima T, Koide K, Fukatsu N, Ohashi T, Iwahara H, A new hydrogen sensor for molten aluminum, *Sensor Actuat B*, **1993**, 14(1-3), 697-699.
25. Yajima T, Iwahara H, Koide K, Yamamoto K, CaZrO<sub>3</sub>-type hydrogen and steam sensors: trial fabrication and their characteristics, *Sensor Actuat B*, **1991**, 5, 145-147.
26. Iwahara H, Kagaku Kogyo, **1993**, 44, 846.
27. Iwahara H, Hibino T, *Proc. Electrochem Soc.*, **1993**, 93, 464.
28. Hibino T, Iwahara H, BaCeO<sub>3</sub> based proton conductor sensitive to ethanol, *Chem. Lett.*, **1992**, 1225-1228.
29. Hibino T, Iwahara H, Amperometric – type sensor for CO<sub>2</sub> using BaCeO<sub>3</sub> based ceramic, *Chem. Lett.*, **1992**, 1221-1224.

30. Iwahara H, Technological challenges in the application of proton conducting ceramics, *Solid State Ionics*, **1995**, 77, 289-298.
31. Miura N, Yamazoe N, Development of new chemical sensors based on low-temperature proton conductors, *Solid State Ionics*, **1992**, 53, 975-982 .
32. Jin L T, Zhao G Z, Fang Y Z, *Chin. J Chem.*, **1994**, 12, 343.
33. Kuwata S, Miura N, Yamazoe N, A Solid-State amperometric oxygen sensor using Nafion membrane operative at room temperature, *Chem. Lett.*, **1988**, 1197-1200.
34. Alberti G, Casciola M, Palombari R, Amperometric sensor for carbon monoxide based on solid state protonic conduction, *Solid State Ionics*, **1993**, 61, 241-244.
35. Alberti G, Casciola M, Palombari R, Potentiometric sensor for oxygen based on O<sub>2</sub>/H<sub>2</sub> mixed potential of a composite Pt-metal hydride electrode, *Solid State Ionics*, **1992**, 52, 291-295.
36. De Angelis L, Maimone A, Modica L, Alberti G, Palombari R, A new hydrogen sensor with pellicular Zr phosphate as proton conductor, *Sensor Actuat B*, **1990**, 1, 121-124.
37. Alberti G, Casciola M, Palombari R, *Elektrokhimiya*, **1993**, 29, 1436.
38. Chowdhari B V R, *Solid State Ionics: Materials and Applications*, World Science, Singapore, (**1992**) 247.
39. Kim Y, Song M, Kim K, Park S, Min S, Rhee H, Nafion/ZrSPP composite membrane for high temperature operation of PEMFCs, *Electrochimica Acta*, **2004**, 50, 645-648.
40. Yaroslavtsev A B, Modification of solid state proton conductors, *Solid State Ionics*, **2005**, 176, 2935-2940.
41. Boilot J P, Barboux P, Carriere D, Lhalil K, Moreau M, Proton conductivity of colloidal nanometric zirconium phosphates, *Solid State Ionics*, **2003**, 162, 185-190.
42. Alberti G, Bracardi M, Casciola M, Ionic conduction of  $\gamma$ -titanium phosphate in hydrogen and alkali metal salt forms, *Solid State Ionics*, **1982**, 7, 243-247.
43. Stenina I A, Aliev A D, Glukhov I V, Spiridonov F M, Yaroslavtsev A B, , Cation mobility and ion exchange in acid tin phosphate, *Solid State Ionics*, **2003**, 162, 191.
44. Tarnopolsky V A, Stenina I A, Yaroslavtsev A B, Cation mobility in acid zirconium and tantalum phosphates and ion-exchange products

- ( $\text{Na}_x\text{H}_{1-x}\text{Ta}(\text{PO}_4)_2 \cdot n\text{H}_2\text{O}$  and  $\text{Na}_y\text{H}_{2-y}\text{Zr}(\text{PO}_4)_2 \cdot n\text{H}_2\text{O}$ ), *Solid State Ionics*, **2001**, 145, 261-264.
45. Clearfield A, Role of ion exchange in solid-state chemistry, *Chem. Rev.*, **1988**, 88, 125.
  46. Hogarth W H J, Muir S. S, Whittaker A K, Diniz da Costa J C, Drennan J, Lu(Max) G Q, Proton conduction mechanism and the stability of sol-gel titanium phosphates, *Solid State Ionics*, **2007**, 177, 3389-3394.
  47. Alberti G, Casciola M, Costantino U, Vivani R, Layered and pillared metal(IV) phosphates and phosphonates, *Adv Mater.*, **1996**, 8, 291-303.
  48. Anderson S, Lundsgeard J, Malling J, Jensen J, Investigation of the dc conductivity of the proton conductors: hydrated antimonite oxide and hydrated  $\alpha$ -zirconium hydrogenphosphate, *Solid State Ionics*, **1984**, 13, 81-85.
  49. Clearfield A, Layered and three-dimensional phosphates of tetravalent elements, *Eur. J. Inorg. Chem*, **1991**, 22, 17-26.
  50. Clearfield A, Berman J R, On the mechanism of ion exchange in zirconium phosphates-XXXIV. Determination of the surface areas of  $\alpha$ -Zr(HPO<sub>4</sub>)<sub>2</sub>·H<sub>2</sub>O, *J Inorg.Nucl. Chem.*, **1981**, 43, 2141-2142.
  51. Casciola M, Bianchi D, Frequency response of polycrystalline samples of  $\alpha$ -Zr(HPO<sub>4</sub>)<sub>2</sub>·H<sub>2</sub>O at different relative humidities, *Solid State Ionics*, **1985**, 17, 287-293.
  52. Casciola M, Costantino U, Relative humidity influence on proton conduction of hydrated pellicular zirconium phosphate in hydrogen form, *Solid State Ionics*, **1986**, 20, 69-73.
  53. Alberti G, Casciola M, Constantino U, Radi R, *Gazz. Chim. Ital*, **1979**, 109, 421.
  54. Alberti G, Casciola M, Constantino U, Levi G, Riccardi G, On the mechanism of diffusion and ionic transport in crystalline insoluble acid salts of tetravalent metals –I: Electrical conductance of zirconium bis (monohydrogenorthophosphate) monohydrate with a layered structure, *J Inorg. Nucl. Chem.*, **1978**, 40(8) 533-537.
  55. Kreuer K D, Proton conductivity: Materials and applications, *Chem. Mater.*, **1996**, 8, 610-641.
  56. Alberti G, Casciola M, Constantino U, *Solid State Protonic Conductors II*, Odense University Press, Odense, Denmark (**1985**) 215.

57. Hamlem R P, Ionic conductivity of zirconium phosphate, *J Electrochem Soc*, **1962**, 109 (8), 746-749.
58. Alberti G, Torracca E, Crystalline insoluble acid salts of polyvalent metals and polybasic acids - VI: Preparation and ion-exchange properties of crystalline titanium arsenate, *J Inorg. Nucl. Chem.*, **1968**, 30, 3075-3080.
59. Anderson E, Anderson I, Moller K, Simonsen K, Skou E, On the preparation of iodine pentafluoride, *Solid State Ionics*, **1982**, 7, 301-302 .
60. Sadaoka Y, Matsuguchi M, Sakai Y, Mitsui S, Electrical properties of zirconium bis(monohydrogen phosphate) monohydrate and its related compounds in a humid atmosphere, *J Meter. Sci.*, **1987**, 22, 2975-2982.
61. Alberti G, Casciola M, Constantino U, DiGregorio F, *Solid State Ionics*, 32-33, **1989**,40.
62. Zaidi S M, Mikhailenko S D, Robertson G P, Guiver M D, Kaliaguine S, Proton conducting composite membranes from polyether ether ketone and heteropolyacids for fuel cell applications, *J Membr. Sci.*, **2000**, 173, 17-34.
63. Rodriguez E, Jimenez J, Jimenez A, Maireles P, Ramos J, Jones D, Roziere J, Proton conductivity of mesoporous MCM type of zirconium and titanium phosphates, *Solid State Ionics*, **1999**, 125,407-410.
64. Casciola M, Costantino, Damico D S, *ac* Conductivity of cerium(IV) phosphate in hydrogen form, *Solid State Ionics*, **1988**, 28, 617-621
65. Le M V, Tsai D S, Yang C Y, Chung W H, Lee H Y Proton conductors of cerium pyrophosphate for intermediate temperature fuel cell, *ElectrochimicaActa.*, **2011**, 56, 6654– 6660.
66. Onoda H, Inagaki Y, Kuwabara A, Kitamura N, Amezawa K, Nakahira A, Synthesis and electrical conductivity of bulk tetra-valent cerium pyrophosphate, *J Cera. Proc. Res.*, **2010**, 11(3), 344-347.
67. Nicole A, B Simon Mun, Hannah L Ray, Philip N, Ross Jr., Jeffrey B, Neaton, Lutgard C, De Jonghel, Structure and electronic properties of cerium orthophosphate: Theory and experiment, *Phys. Rev. B*, **2011**, 83, 205104-205107.
68. Gomez del Moral A, Fagg D P, Chinaro E, Abrantes Jao C C, Juraó J M, Mather G C, Impedance analysis of Sr-substituted CePO<sub>4</sub> with mixed protonic and p-type electronic conduction, *Cera. Int.*, **2009**, 35, 1481-1486.

69. Failong D, Zhongfang L, Wang S, Wang Z, Synthesis and characteristics of proton-conducting membrane based on cerium sulphenyle phosphates and poly(2, 5-benzimidazole) by hot-pressing method, *Int. J. Hydro. Enregy*, **2011**, 36, 11068-11074.
70. Khan A A, Inamuddin, Cation-exchange kinetics and electrical conductivity studies of an ‘organic-inorganic’ composite cation-exchanger: Polypyrrole-Th(IV) phosphate, **2007**, 105(5), 2806-2815
71. Beena B, Chudasama U, Transport properties in a mixed inorganic ion exchanger zirconium phosphomolybdate - in comparison to its single salt counterparts, *Bull Mater Sci*, **1996**, 19, 405.
72. Beena B, Pandit B, Chudasama U, Transport properties of organic derivatives of zirconium molybdate, *Indian J Eng. Mater. Sci.*, **1998**, 5, 77.
73. Parikh A, Chudasama U, A comparative study of the proton transport properties of metal (IV) tungstates, *Proc. Ind. Acad. Sci.*, 115, **2003**, 1.
74. Patel H, Parikh A, Chudasama U, A comparative study of proton transport properties of metal (IV) tungstates and their organic derivatives, *Bull Mater Sci.*, **2005**, 28, 137-144.
75. Patel H, Chudasama U, A comparative study of the proton transport properties of zirconium(IV) phosphonates, *Bull. Mater. Sci.*, 29(7), 665-671.
76. Casciola M, Costantino U, Relative humidity influence on proton conduction of hydrated pellicular zirconium phosphate in hydrogen form, *Solid State Ionics*, **1986**, 20, 69-73.
77. Hammas I, Horchani-Kaifer K, Ferid M, Conduction properties of condensed lanthanum phosphates;  $\text{La}(\text{PO}_3)_3$  and  $\text{LaP}_5\text{O}_{14}$ , *J Rare Earths*, **2010**, 28(3), 321-328.
78. Alberti G, Costantino U, Polambari R, *First International Conference on Inorganic Membranes*, Montpellier, France, **1989**, 25.
79. Pauling L, Atomic radii and interatomic distances in metal, *J Am. Chem. Soc.*, **1947**, 69(3), 542-553.